



sets now exist measuring changes in host gene regulation [15] and gut microbial composition [20,35] as a response to the fresh-/salt-water transition and to different feed types. However, these datasets have so far only been analyzed individually with traditional methods. In this article, we aim to study interactions between the salmon and its gut microbiota by data integration.

Previous studies that have attempted to investigate holobiont interactions by generating large-scale omics data from both the host and the associated microbiota have been limited by a deficit of computational tools and methods [30]. Networks naturally describe interactions, and network-based computational methods have therefore dominated efforts to tease apart such interactions. [19] used networks to identify host gene modules and correlated these with bacterial community variables and individual operational taxonomic units (OTUs) of the microbiome. TransNet (Transkingdom Network, [34] infers unweighted networks of bacterial OTUs and host genes separately. The method relies on differential expression analysis to reduce the number of nodes in the network, followed by network inference, module identification and finally identifies causal host and microbial nodes using high bipartite betweenness centrality in transkingdom networks. Attempts have also been done to infer structural host-microbiota interaction networks by predicting complexes formed between host proteins and microbial components [16,4]. Here, we develop and apply a network-based dimensionality reduction method for analysing holobiont omics data. The pipeline infers networks for both the host and the microbiota and provides robust predictions of putative Interactions between them. The framework is largely automatic requiring little manual tinkering and is based on weighted networks that do not depend on arbitrary thresholds on correlation [18]. The developed pipeline is then applied to the previously described salmon gut omics datasets.

## 2. Results

To gain insight into host-microbiota interactions in the Atlantic salmon (*Salmo salar*) gut, we performed an integrative analysis of RNA-seq data from the gut epithelial tissue [15] and 16S rRNA amplicon sequencing data from the gut content [20,35] collected from a long-term feeding trial (Supplementary Fig. 1). The trial spanned fresh- and salt-water life stages and included feeds low (VO – Vegetable Oil) and high (FO – Fish Oil) in long-chain polyunsaturated fatty acids (LC-PUFAs), resembling food availability in rivers and the ocean, respectively. After preprocessing (see Methods), the dataset contained matching measurements of 37,408 host genes and 296 microbiotic OTUs in 147 samples.

### 2.1. A novel method for holobiont interaction analysis

We developed a computational pipeline for integrating host and microbiota omics datasets based on weighted network analysis (Supplemental Fig. 2). We infer networks for each omics dataset separately using the Weighted Gene Co-expression Network Analysis (WGCNA) method [24]. Briefly, networks are soft-thresholded to reach an approximate scale free topology, network modules are detected using the robust weighted Topological Overlap Measure (wTOM) [42] and hierarchical clustering, and the first principle component is used as a representative profile for each module (generally referred to as host/microbiota Module Eigennodes – hME/mME, or, specifically as eigengenes/eigenOTUs). We then assign functional roles at the network module level via function enrichment analysis, while high resolution analysis of the individual modules is enabled through ranking of genes and OTUs (i.e. nodes) by network centrality. Finally, we devised an integrated heatmap analysis to visualize and predict putative transkingdom

interactions by correlating module eigennodes between the two networks, and by associating these predicted interactions to host traits and other external variables such as feed and water type.

### 2.2. Fresh-/salt-water transition dominates omics associations

Our analysis of the host gene co-expression network revealed 171 distinct gene modules with low correlation between modules (between host Module Eigengenes – hMEs) and high correlation between genes within the same module (Supplementary Fig. 3). These modules contained 13,525 genes (Supplementary table 1). The microbiota network contained five modules harboring 95 OTUs (Supplementary table 2). Although these modules were distinct, they were clearly clustered into two negatively correlated groups (Supplementary Fig. 4). The relatively large fraction of genes (64%) and OTUs (68%) not included in modules indicates that many genes and bacterial species have largely unique variation in abundance profiles across the individual fish sampled in this study. In an unsupervised framework, such genes/OTUs are assumed to largely make up genes that do not vary (e.g. housekeeping genes) or that display variation not relevant for the processes studied in these data sets.

We developed a visualization scheme where gene module expression, transkingdom putative interactions and omics correlations to host traits and external variables are assembled into an integrated Heatmap Analysis of Holobiont Interactions (iHAHI, Fig. 1). This analysis clearly shows that the fresh-/salt-water transition explains much of the structure in both the host and microbial network. The 50 host modules with a significant association to both external variables and microbiota modules ( $p < 0.05$ ) are broadly divided into two groups: group 1 contained modules of genes that to some degrees have higher expression in saltwater (i.e. positively correlated to WaterSW – Salt Water, and to Day, which is inherently linked to water type), whereas group 2 primarily have higher expression in freshwater (i.e. negatively correlated to WaterSW). Notably, the two largest host modules (represented by host Module Eigengene 1 – hME1 – and 2 – hME2) have the strongest negative/positive association to saltwater, respectively. Some of the strongest associations between host and microbial modules are also observed for these two modules. This is explained by the fact that microbial modules also are heavily influenced by the fresh-/salt-water transition: microbial modules 1 and 2 (microbial Module EigenOTU 1 – mME1 – and 2 – mME2) contain OTUs abundant in saltwater, while modules 3, 4 and 5 contains genes abundant in fresh water (Supplementary Fig. 4).

Since many host and microbiota modules correlate with the fresh-/salt-water transition, it is difficult to distinguish actual host-microbial interactions in these modules from scenarios where both host and microbial modules are independently explained by water-type. In order to gain further insight into this, we investigated gene function enrichment and OTU content in host-microbiota module-pairs abundant in saltwater (hME2 and hME3 and their correlation with mME1 and mME2) and in freshwater (hME1, hME56, hME76 and hME79 and their correlation with mME 3 and mME4).

#### 2.2.1. Host-microbiota modules abundant in saltwater

Host module 2 was highly enriched for processes such as intracellular protein transport ( $p = 1e-30$ ), lipid synthesis processes such as phosphatidylethanolamine biosynthetic process ( $p = 2.2e-12$ ), cholesterol biosynthetic process ( $p = 3.2e-10$ ), triacylglycerol biosynthesis process ( $p = 3.2e-10$ ), long-chain fattyacyl-CoA biosynthetic process ( $p = 5.9e-8$ ) and regulation of lipid storage ( $2e-7$ ) while host module 3 was also enriched for lipid related processes such as triglyceride homeostasis ( $p = 3.2e-4$ ), lipid oxidation ( $5.3e-4$ ) and lipid catabolic process ( $1.1e-3$ )

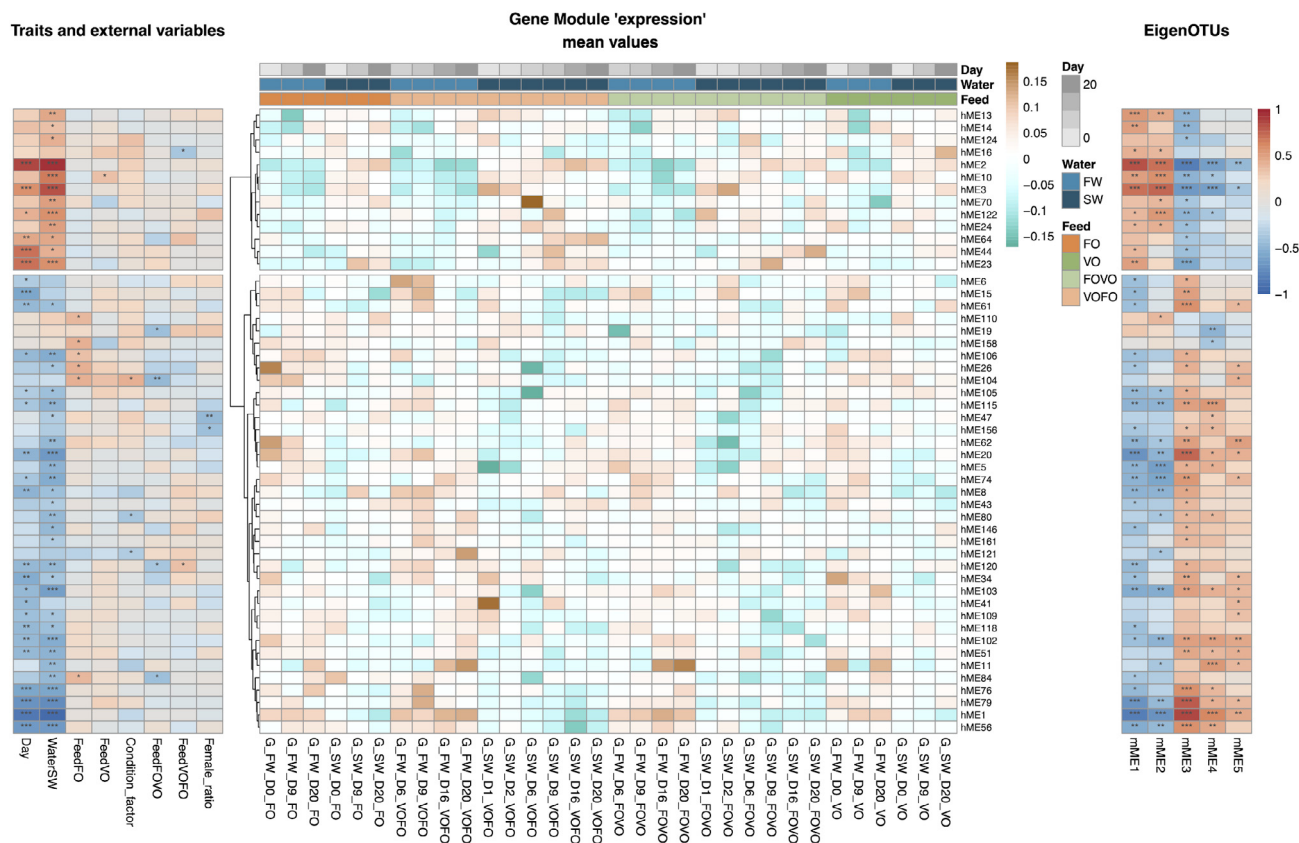


**Fig. 1.** Integrated heatmap. The figure shows correlations between the host gene expression module eigengenes (hME) and the microbiome abundance module eigenOTUs (mME), as well as between hME and host traits and external variables. The central heatmap shows the ‘expression’ of the hMEs, where rows are hMEs and columns are sample groups (i.e. mean of replicates). Sample groups are ordered by feed type, then water type and finally by day. The right heatmap shows correlation strengths between hMEs and mME, while the left heatmap shows correlation strengths between hMEs and host traits/external variables. Correlations are computed across sample groups. A strong positive correlation is represented by deep red, and a strong negative correlation by deep blue. A correlation of 0 is white. Statistical significance of the correlations as indicated with stars: \*  $p \leq 0.05$ , \*\*  $p \leq 0.01$ , \*\*\*  $p \leq 0.001$ . (For interpretation of the references to colour in this figure legend, the reader is referred to the web version of this article.)

(Supplementary table 3). These processes are in line with the function of gut epithelial cells given high availability of LC-PUFAs. Microbial module 1 contains a majority of Firmicutes (37 of 45), which generally dominates the gut in salt water, but also contains Proteobacteria (4), Actinobacteria (3) and Cyanobacteria (1) (Supplementary Fig. 5). Many OTUs in this module persist across the freshwater-saltwater transition, although more highly abundant in salt- than in fresh-water, and includes as highly central nodes all four OTUs constituting the “stable core gut microbiota” previously discussed by [35] (Supplementary Fig. 5). Microbial module 2 has a different OTU profile, containing Bacteroidetes (6 of 22), Proteobacteria (6) Fusobacteria (4), Cyanobacteria (3) and Firmicutes (3). Deeper taxonomic assignments at the genus level identified many taxa associated with fresh and marine water environments (i.e. Planktothrix, Aeromonas etc), but also indicated a prevalence of Bacteroides-like populations, which are widely recognized in gastrointestinal ecosystems for their fermentative capabilities of host and plant-derived glycans [28] (Supplementary Table 2).

### 2.2.2. Host-microbiota modules abundant in freshwater

Host module 1 is highly enriched in extracellular matrix disassembly ( $p < 5.6e-27$ ) including collagen catabolic process ( $p < 6.4e-19$ ). Microbial module 3 contains Proteobacteria (7), which generally dominates the gut in fresh water, but also Actinobacteria (3), Firmicutes (2), Cyanobacteria (1) and the only Synergistetes in the data set. Microbial module 4 is also dominated by Proteobacteria (7 of 8) and contains one Bacteroidetes. Both microbial modules

were dominated by taxa frequently observed in water-bourne habitats with only limited examples of host-associated microbiota (i.e. Enterococcus).

Taken together, these results indicate that the environment is the primary driver of selection on gut microbiota with large numbers of genes and OTUs differentially abundant between fresh- and salt-water. Still, significant host-microbial associations related to feed, sex and growth does exist, suggesting that diet or host metabolism may play some role in shaping the co-occurrence of associated host-microbiota modules.

### 2.3. Host-microbial associations related to feed, sex and growth exists

Beyond the large effect that the fresh/salt water-transition had on both host gene expression and gut microbiota, we also identified significant associations between host gene expression and microbial communities that are linked to feed types (Feed), sex (Female\_ratio) and fish weight and length (Condition\_factor, see Methods) (Fig. 1). Compared to the large effects of the fresh/salt water transition, these correlations were much weaker, involved small host modules, and generally did not co-vary with water type. Nevertheless, many biological meaningful connections are evident. For example, host module hM47 is associated with the sex of the fish and contains a sprouty-related 2C gene known to have sex-biased gene expression in other fish [38].

All four feed categories (FO, VO, FO → VO, and VO → FO) had at least one significant correlation to a host-module and to a

microbial module (Fig. 1). These host modules consisted of genes linked to functions such as ion transport (hM10, hM104), fatty acid binding (hM10), apoptosis (hM120), and muscle function (hM10), but also various genes associated with anti-inflammatory pathways (Supplementary table 1). For example, the switch of diet from FO to VO was particularly strongly associated with expression of hM104, which contains the ankyrin-3 gene (*ank3*) that alters Na-K-ATPase activity during chronic intestinal inflammation [37]. In line with this, increased levels of n-3 LC-PUFA (DHA and EPA) in the feed have been shown to activate anti-inflammatory processes in the gut in both mammals and fish [29,8].

The switch of diet from VO to FO was associated with hME16 which contains interferons regulatory factor genes (*irf-3* and *irf-7*), signal transducer and activator of transcription 1 gene (*stat-1*) and interferon-induced very large GTPase 1 gene (*gvinp-1*) involved in innate and adaptive immune responses. The interferon signalling involves *irf-3* and *irf-7* which regulates the transcription of type 1 interferons (T1ifn) and leads to phosphorylation of Stat-1 and Stat-2 [14,26]. The Stat-1 and -2 dimerize and form a complex, which enters the nucleus and affects transcription of interferon-stimulated genes (ISGs). The genes of hME16 were negatively correlated to VOFO, supporting a previous study that dietary inclusion of LC-PUFA decreases stimulated-interferon production [17]. An alternation of T1IFN signalling in host could change the composition of commensal microorganisms in the host intestine, and conversely the intestinal microbial community also plays an important role for maintaining a stable T1IFN production at mucosal surfaces [14]. Furthermore, a study in mice also showed that the colonisation of microbiota is important for the development of T1IFN signalling systems at early stages [13].

Host module 16, associated with VOFO and two microbial modules (mME1 and mME2), contains a butyrate response factor 1 gene (NCBI locus identifier 100195422). This gene is known to be regulated by changes in butyrate levels in colorectal cells in mammals [27]. Interestingly, within microbial module 1 we identified an OTU affiliated to *Faecalibacterium* (OTU\_45), a renowned butyrate-producing beneficial bacterium in the mammalian gut that is commonly associated with gastrointestinal health [12]. Closer inspection of OTU45 and butyrate response factor 1 demonstrated a stronger correlation between these than between the modules themselves ( $p = 0.001$ ). The predicted hM16-mME1 interaction hence represents an interesting candidate for a functional link between microbial metabolism and host-gene regulation.

#### 2.4. Host-microbial associations after removing large effects

Because the fresh-to-salt water transition in the dataset has an overwhelmingly large effect on gene expression and microbial composition, it is plausible that other associations have remained undiscovered in the initial analysis described above. To gain further insight into host-microbiota associations, we therefore reran our pipeline on omics data subjected to a method designed to remove large effects (see Methods). Interestingly, this revealed a large number of small modules for both the host (123 host modules, Supplementary figures 6) and microbiota networks (89 microbiota modules, Supplementary figure 7). These modules included a large proportion of genes (586 of 1492 genes, Supplementary table 4) and OTUs (156 of 228 OTUs, Supplementary table 5) not assigned to modules in the initial analysis, and thus represented a potential for new discoveries.

Fig. 2 clearly shows that removing large effects deemphasized association related to water type and sampling day, and instead revealed several strong associations ( $p < 0.01$ ) involving nine host modules, 17 microbiota modules and host variables linked to feed and sex. Here we focus on modules with associations linked to both VO and FO feeds: Host module 2 is enriched for genes with a role in

the cholesterol biosynthetic process ( $p = 1E-30$ , Supplementary table 6), which is the same enrichment as for genes highly expressed in salt water in the initial analysis (host module 2 in Fig. 1). However, unlike in the initial analysis, host module 2 after removing large effects (Fig. 2) has a strong association to feed, with a positive correlation to VO feed and a negative correlation to FO feed. The same feed association can be found for host module 58. A higher requirement for endogenous cholesterol has previously been suggested to be an effect of dietary VO which is naturally devoid of cholesterol [21,15]. Further supporting this, host module 58 includes a scavenger receptor class B type I gene (*sr-bi*) that suggest a higher requirement of cholesterol absorption in the intestine in VO [6,3]. Furthermore, host module 39, displaying the reverse association to feed (negative correlation to VO feed and positive to FO feed), is enriched for positive regulation of epithelial to mesenchymal transition ( $p = 0.00016$ ). Host module 39 includes two genes, beta,beta-carotene 9',10'-oxygenase-like (*bco2*) involved in cleavage of carotenoids and lecithin retinol acyltransferase-like (*lrat*) involved in esterification of carotenoids. The higher expression of genes involved in carotenoid metabolism could be linked to LC-PUFA levels in FO. A previous study has shown that sterol esters containing LC-PUFA have higher bioavailability than vegetable oil fatty acid esters [23]. Multiple microbial taxa were also observed to associate with host modules 2, 58 and 39, including several lineages affiliated to gastrointestinal commensals such as *Paraeggerthella* (OTU\_230, mME5) [25] and those linked to fermentation and/or fatty acid utilization (e.g. *Tepidimicrobium*: OTU\_311, mME5 and OTU\_257, mME58) [40]. However, it must be noted that little phenotypic and genomic information exists for these genera in any environment notwithstanding the salmon gut for which there exists no data. This current lack of data for microbial function makes it problematic to infer definitive predictions of metabolic functions based on our 16S rRNA data and to connect their putative associations to host modules. It is hoped that these knowledge gaps will quickly be filled as improvements to microbiome genome inventories are occurring at a rapid pace.

Taken together, we successfully removed the dominating effect of water type and sampling day from the host and microbiota omics data, and then showed that our network-based framework could reveal hitherto undiscovered host-microbiota-feed associations in this data.

### 3. Discussion

Previous studies have shown that both changes in feed composition and migration between fresh- and sea-water environments remodel salmon gut tissue function as well as gut microbial composition [15,21,22,41] Yet, during these significant events there is little to no knowledge about potential interconnections between the microbial community functions and salmon gene regulation and gut physiology. To close this knowledge gap there is a pressing need to co-analyze host and microbiome responses in a unified manner.

Here we used matching host gene expression and microbial level measurements to search for host-microbiota interactions using a novel computational method combining network-based dimensionality reduction for analysing holobiont omics data and an integrated Heatmap Analysis of Holobiont Interactions (iHAHI) for visualizing putative interactions. Although this method was applied herein to a salmon dataset, it can be applied to any holobiont dataset in animals or plants. In fact, the R code is available as modules (R Markdown files) each performing one step in the computational analysis pipeline (Supplementary Fig. 2) including generating all figures presented as part of this article. Using this pipeline, we find that it is difficult to separate salmon host-



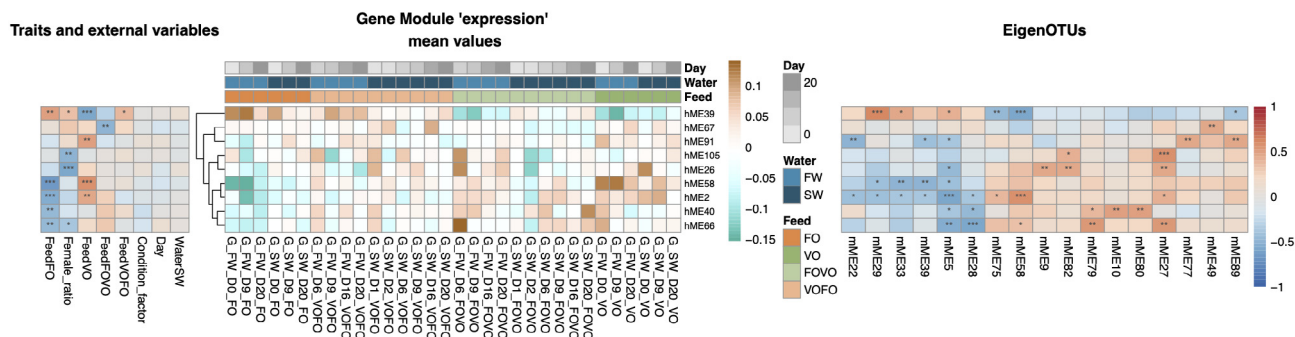


**Fig. 2.** Integrated heatmap with large effects removed. The figure shows correlations between the host gene expression module eigengenes (hME) and the microbiome abundance module eigenOTUs (mME), as well as between hME and host traits and external variables. The central heatmap shows the ‘expression’ of the hMEs, where rows are hMEs and columns are sample groups (i.e. mean of replicates). Sample groups are ordered by feed type, then water type and finally by day. The right heatmap shows correlation strengths between hMEs and mME, while the left heatmap shows correlation strengths between hMEs and host traits/external variables. Correlations are computed across sample groups. A strong positive correlation is represented by deep red, and a strong negative correlation by deep blue. A correlation of 0 is white. Statistical significance of the correlations as indicated with stars: \*  $p \leq 0.05$ , \*\*  $p \leq 0.01$ , \*\*\*  $p \leq 0.001$ . (For interpretation of the references to colour in this figure legend, the reader is referred to the web version of this article.)

microbiota interactions from independent effects in the host and the microbiota both caused by the fresh-/salt-water transition. Although in seawater, we observed OTUs affiliated to the *Bacteroides*, which are well recognized for their commensal activity within gastrointestinal ecosystems. In the context of dietary changes, previous traditional single-omics analysis showed that while host gene regulation plays a role in adopting salmon to different LC-PUFA availability, the gut microbiota composition seems not to play a major role. In this study we similarly observed correlations between host gene expression and feed, however by introducing an additional layer of data encapsulating gut microbiome composition, we revealed putative interactions that arise from possible microbiome butyrate-producing activity. Collectively, our data therefore suggests that perhaps overlooked dietary-linked commensal populations that are critical to mammalian nutrition and wellbeing (such as *Bacteroides* and *Faecalibacterium*) are also important within salmon. Finally, we show that when large effects are removed from our analysis we increase the resolution of network associations, revealing previously hidden and possibly important biological interactions.

Our method for detecting robust interactions between host and microbiota was here used to find correlated modules of host genes and microbiota OTUs. While individual host genes and microbiota OTUs might still exhibit signals of interactions, the use of microbial taxa as a marker as opposed to microbial gene function may well mask many critical functional interactions that exist between metabolic pathways that have not yet been attributed to taxonomically-described salmon gut microbiota. In addition, the presence of an OTU or gene/pathway does not automatically infer activity. The current lack of data for microbial function makes it problematic to infer definitive predictions of metabolic functions based on 16S rRNA data and to connect their putative associations to host modules. It is hoped that these knowledge gaps will quickly be filled as improvements to microbiome genome inventories are occurring at a rapid pace. Irrespective, we argue that our method easily can encompass host and microbial gene expression data once representative datasets become available for salmon.

## 4. Materials & methods

### 4.1. Materials

The omics data were generated using 367 samples from a long term feeding trial of farmed Atlantic salmon (*Salmo Salar*) (for experimental design see [Supplementary Fig. 1](#)). The salmon were

raised on two contrasting diets: one vegetable oil diet (VO) with low amounts of long chain polyunsaturated fatty acids (LC-PUFA), containing a 1.8:1 ratio of linseed oil and palm oil, and one fish oil diet (FO) high in LC-PUFA, based on fish oil from the North Atlantic [15,35]. The fish were switched to the contrasting diet (VO to FO and vice versa) at ~ 50 g in freshwater, and tissue samples were taken 1, 2, 5, 9, 16 and 20 days after the diet switch ([Supplementary Fig. 1b](#)). The control fish on the original diets was put through the smoltification process and then transferred to seawater. Another diet switch trial was performed in seawater when the fish reached ~ 200 g, and tissue samples were again taken at 1, 2, 6, 9, 16 and 20 days after the diet switch. Samples of the control tanks were taken at 0, 5, 9 and 20 days after diet switch in freshwater and at 0, 9 and 20 days in seawater.

Atlantic salmon RNA-seq reads from the gut epithelial tissue samples were taken from [15] and are available in the European Nucleotide Archive (ENA) as project PRJEB24480. Transcript expression values were quantified using Salmon [32]. Corresponding gut microbiota 16S rRNA amplicon sequencing reads were taken from [35] and are available in the Sequence Read Archive (SRA) under accession number SRP119730. OTUs were identified from 16S sequences using the USEARCH pipeline with 97% sequence identity. Classifications were done with the R-package *microclass*.

### 4.2. Methods

The developed computational analysis pipeline is visualized in detail in [Supplementary Fig. 2](#).

#### 4.2.1. Data preprocessing

Transcript expression counts were summed for each gene. Expression values were normalized across samples using the Trimmed mean of M values (TMM)-method [33], and log<sub>2</sub>-transformed. Genes with expression levels below 1.0 in all samples and/or with a standard deviation less than 0.15 were removed before network inference. This reduced the number of genes from 48,057 to 37,408.

We retained OTUs that contribute at least 0.005% of the total microbial abundance. This reduced the number of OTUs from 1152 to 296 and the number of zeros in the abundance table by 50%. OTU abundances was normalized using the Cumulative Sum Scaling (CSS) method from the Bioconductor package *metagenome-Seq*, which by default log<sub>2</sub>-transforms the data.

Samples were first normalized with a min-max normalization (Cao, Stojkovic, and Obradovic 2016) and then clustered with average distance to identify outliers. Two samples were removed: RNA-seq sample G\_FW\_D20\_FOVO\_2 and 16S sample G\_FW\_D9\_FOVO\_2.

#### 4.2.2. Network inference

For network inference, we used the Weighted Gene Co-expression Network Analysis (WGCNA) R package [24] and the function *blockwiseModules* with the bicor correlation measure and parameters `maxBlockSize = 10000`, `networkType = "signed"`, `TOMType = "signed"`, `corType = "bicor"`, `maxPOutliers = 0.05`, `replaceMissingAdjacencies = TRUE`, `pamStage = F`, `deepSplit = 4`, `minModuleSize = 2`, `minKMEtoStay = 0.5`, `minCoreKME = 0.5`, `minCoreKMESize = 2`, `reassignThreshold = 0` and `mergeCutHeight = 0.4/0.5` (for microbiota/host respectively).

Our analysis relies heavily on network modules, and hence the parameters related to module detection and trimming influence the results. Briefly, `deepSplit` controls the sensitivity of the module detection approach by hierarchical clustering, with a value of 1 being the least sensitive and 4 being the most sensitive. `minModuleSize` controls the minimum size of modules in the clustering step. Nodes with a correlation to the module eigennode (KME) lower than `minKMEtoStay` are trimmed from the module, and the module is deleted if it does not have a core of at least `minCoreKMESize` nodes (with core nodes being defined as having a KME greater than `minCoreKME`). Finally, different modules with eigennodes that correlate above the `1 - mergeCutHeight` threshold are merged. Note that the final modules can be smaller than `minModuleSize` due to trimming (but not smaller than `minCoreKMESize`), and that they can include nodes with a KME lower than `minKMEtoStay` due to module merging. Our parameters were set to detect highly correlated and potentially small modules initially, thus not missing interesting profiles displayed by few genes/OTUs, and then to apply an aggressive merging threshold to avoid dealing with highly redundant modules in downstream analysis.

Network centrality of genes and OTUs were calculated using the function *intramodularConnectivity.fromExpr*.

The removal of large-effect variables using the PC-correction method available in the R-package *sva* [31], which is a method developed for co-expression networks, is implemented in the code. The number of latent variables to be removed is estimated using the permutation-based approach implemented in the *num.sv* function and the variables can then be regressed out using the function *sva\_network*.

#### 4.2.3. Host variables

We correlated a set of host variables/traits with the omics data including day, feed, water type, sex, weight and length. The categorical feed-variable has four values: vegetable oil (VO), fish feed (FO) and the two transitions from VO to FO (VOFO) and from FO to VO (FOVO). To allow correlation analysis we expanded this variable into four new binary variables using “one hot encoding” with each new variable taking values 1 (e.g. VO) and 0 (e.g. not VO). Instead of using host weight and length directly, we calculated the condition factor (CF) of the fish, which is considered an indirect measure of fish fatness [5,2]. The new variable CF is a continuous variable:

$$CF = \frac{10^N \cdot W}{L^3}$$

where *W* is the weight of the fish in grams, *L* is the length of the fish in millimeters and *N* is a constant used to bring the range of output values close to 1. The value of *N* differs from *N* = 2 [2] to *N* = 5 [5]. Here we used a value of *N* = 4 which gives the expected range.

#### 4.2.4. Integrated heatmap analysis of holobiont interactions

We devised and implemented a heatmap analysis to visualize and predict putative holobiont interactions by integrating host and microbiota module eigennodes with host variables (see Figs. 1 and 2). To obtain reliable estimates of the significance of associations between host eigengenes and both host variables and eigen-OTUs, correlations were computed after averaging the expression/abundance values of replicates. Correlations and p-values were computed using the R function *cor.test* using the Spearman correlation for the ordinal day-variable and the default Pearson correlation for all other variables.

#### 4.2.5. Gene ontology enrichment

The R package TopGO [1] was used to test for gene function enrichment.

#### 4.2.6. Code availability

The R-markdown files and R-scripts are available at: [https://gitlab.com/M.strand/wgcna\\_host\\_microbiome](https://gitlab.com/M.strand/wgcna_host_microbiome).

### CRedit authorship contribution statement

**Marius A. Strand:** Methodology, Software, Formal analysis, Data curation, Writing - original draft, Visualization. **Yang Jin:** Investigation, Writing - review & editing. **Simen R. Sandve:** Conceptualization, Investigation, Writing - review & editing, Supervision, Funding acquisition. **Phil B. Pope:** Conceptualization, Investigation, Writing - review & editing, Supervision, Funding acquisition. **Torgeir R. Hvidsten:** Conceptualization, Validation, Writing - original draft, Supervision.

### Acknowledgements

We are grateful for support from The Research Council of Norway (FRIPRO program, PBP and TRH: 250479), the BlueBio COFUND (PBP, TRH and SRS: 311913), and The Research Council of Norway Havbruk program (PBP, TRH and SRS: 300846).

### Appendix A. Supplementary data

Supplementary data to this article can be found online at <https://doi.org/10.1016/j.csbj.2021.01.038>.

### References

- [1] Alexa A, Rahnenführer J, Lengauer T. Improved scoring of functional groups from gene expression data by decorrelating GO graph structure. *Bioinformatics* 2006;22(13):1600–7.
- [2] Aine H, Oehme M, Thomassen M, Terjesen B, Rørvik K. Reduced growth, condition factor and body energy levels in Atlantic salmon *Salmo salar*. *Aquac Res* 2011;42(2):248–59.
- [3] Altmann SW, Davis HR, Yao X, et al. The identification of intestinal scavenger receptor class B, type I (SR-BI) by expression cloning and its role in cholesterol absorption. *BBA* 2002;1580(1):77–93.
- [4] Andrighetti T, Bohar B, Lemke N, Sudhakar P, Korcsmaros T. Microbiolink: an integrated computational pipeline to infer functional effects of microbiome-host interactions. *Cells* 2020;9(5):1278. <https://doi.org/10.3390/cells9051278>.
- [5] Barnham C, Baxter A. Condition Factor, K, for Salmonid Fish. State of Victoria: Department of Primary Industries; 1998.
- [6] van Bennekum A, Werder M, Thuahnai ST, et al. Class B scavenger receptor-mediated intestinal absorption of dietary beta-carotene and cholesterol. *Biochemistry* 2005;44(11):4517–25.
- [7] Bordenstein SR, Theis KR. Host biology in light of the microbiome: ten principles of holobionts and hologenomes. *PLoS Biol* 2015;13(8):e1002226.
- [8] Calder PC. Marine omega-3 fatty acids and inflammatory processes: Effects, mechanisms and clinical relevance. *BBA* 2015;1851(4):469–84.
- [9] Desbonnet L, Clarke G, Shanahan F, Dinan TG, Cryan JF. Microbiota is essential for social development in the mouse. *Mol Psychiatry* 2014;19(2):146–8.
- [10] Dominguez-Bello MG, Godoy-Vitorino F, Knight R, Blaser MJ. Role of the microbiome in human development. *Gut* 2019;68(6):1108–14.
- [11] Egerton S, Culloty S, Whooley J, Stanton C, Ross RP. The gut microbiota of marine fish. *Front Microbiol* 2018;9:873.

- [12] Ferreira-Halder CV, de Faria AVS, Andrade SS. Action and function of *Faecalibacterium prausnitzii* in health and disease. *Best Pract Res Clin Gastroenterol* 2017;31(6):643–8.
- [13] Ganal SC, Sanos SL, Kallfass C, et al. Priming of natural killer cells by nonmucosal mononuclear phagocytes requires instructive signals from commensal microbiota. *Immunity* 2012;37(1):171–86.
- [14] Giles EM, Stagg AJ. Type 1 interferon in the human intestine-A Co-ordinator of the immune response to the microbiota. *Inflamm Bowel Dis* 2017;23(4):524–33.
- [15] Gillard G, Harvey TN, Gjuvsland A, et al. Life-stage-associated remodelling of lipid metabolism regulation in Atlantic salmon. *Mol Ecol* 2018;27(5):1200–13.
- [16] Guven-Maiorov E, Tsai C-J, Nussinov R. Structural host-microbiota interaction networks. *PLoS Comput Biol* 2017;13(10):e1005579.
- [17] Hara Y, Miura S, Komoto S, et al. Exposure to fatty acids modulates interferon production by intraepithelial lymphocytes. *Immunol Lett* 2003;86(2):139–48.
- [18] Horvath S, editor. *Weighted network analysis*. New York, NY: Springer New York; 2011.
- [19] Huang Y, Ma S-F, Espindola MS, et al. Microbes are associated with host innate immune response in idiopathic pulmonary fibrosis. *Am J Respir Crit Care Med* 2017;196(2):208–19.
- [20] Jin Y, Angell IL, Sandve SR, Snipen LG, Olsen Y, Rudi K. Atlantic salmon raised with diets low in long-chain polyunsaturated n-3 fatty acids in freshwater have a *Mycoplasma*-dominated gut microbiota at sea. *Aquacult Environ Inter* 2019;11:31–9.
- [21] Jin Y, Angell IL, Sandve SR, Snipen LG, Olsen Y, Rudi K. Atlantic salmon raised with low LC-n3-PUFA diets in freshwater have a *Mycoplasma* dominated gut microbiota at sea. *Aquac Environ Interact* 2018.
- [22] Jin Y, Olsen RE, Gillard GB, et al. A systemic study of lipid metabolism regulation in salmon fingerlings and early juveniles fed plant oil. *Br J Nutr* 2018;120(6):653–64.
- [23] Jones PJH, Demonty I, Chan Y-M, Herzog Y, Pelled D. Fish-oil esters of plant sterols differ from vegetable-oil sterol esters in triglycerides lowering, carotenoid bioavailability and impact on plasminogen activator inhibitor-1 (PAI-1) concentrations in hypercholesterolemic subjects. *Lipids Health Dis* 2007;6(1):28.
- [24] Langfelder P, Horvath S. WGCNA: an R package for weighted correlation network analysis. *BMC Bioinf* 2008;9:559.
- [25] Lau SKP, Woo PCY, Woo GKS, et al. *Eggerthella hongkongensis* sp. nov. and *eggerthella sinensis* sp. nov., two novel *Eggerthella* species, account for half of the cases of *Eggerthella* bacteremia. *Diagn Microbiol Infect Dis* 2004;49(4):255–63.
- [26] Liu S, Cai X, Wu J, et al. Phosphorylation of innate immune adaptor proteins MAVS, STING, and TRIF induces IRF3 activation. *Science* 2015;347(6227):p. aaa2630.
- [27] Maclean KN, McKay IA, Bustin SA. Differential effects of sodium butyrate on the transcription of the human TIS11 family of early-response genes in colorectal cancer cells. *Br J Biomed Sci* 1998;55(3):184–91.
- [28] Martens EC, Neumann M, Desai MS. Interactions of commensal and pathogenic microorganisms with the intestinal mucosal barrier. *Nat Rev Microbiol* 2018;16(8):457–70.
- [29] Montero D, Torrecillas S, Benítez-Dorta V, Caballero MJ, Izquierdo MS, Zamorano MJ. Effects of dietary vegetable oils on the expression of eicosanoid receptors genes in Senegalese sole (*Solea senegalensis*) intestine. *Aquacult Rep* 2019;15:100201.
- [30] Nyholm L, Koziol A, Marcos S, et al. Holo-Omics: integrated host-microbiota multi-omics for basic and applied biological research. *iScience* 2020;23(8):101414.
- [31] Parsana P, Ruberman C, Jaffe AE, Schatz MC, Battle A, Leek JT. Addressing confounding artifacts in reconstruction of gene co-expression networks. *Genome Biol* 2019;20(1):94.
- [32] Patro R, Duggal G, Love MI, Irizarry RA, Kingsford C. Salmon provides fast and bias-aware quantification of transcript expression. *Nat Methods* 2017;14(4):417–9.
- [33] Robinson MD, Oshlack A. A scaling normalization method for differential expression analysis of RNA-seq data. *Genome Biol* 2010;11(3):R25.
- [34] Rodrigues RR, Shulzhenko N, Morgun A. Transkingdom networks: a systems biology approach to identify causal members of host-microbiota interactions. *Methods Mol Biol* 2018;1849:227–42.
- [35] Rudi K, Angell IL, Pope PB, Vik JO, Sandve SR, Snipen L-G, Drake HL. Stable core gut microbiota across the freshwater-to-saltwater transition for farmed atlantic salmon. *Appl Environ Microbiol* 2018;84(2).
- [36] Rudman SM, Greenblum S, Hughes RC, et al. Microbiome composition shapes rapid genomic adaptation of *Drosophila melanogaster*. *PNAS* 2019;116(40):20025–32.
- [37] Saha P, Manoharan P, Arthur S, Sundaram S, Kekuda R, Sundaram U. Molecular mechanism of regulation of villus cell Na-K-ATPase in the chronically inflamed mammalian small intestine. *BBA* 2015;1848(2):702–11.
- [38] Sharma E, Kunstner A, Fraser BA, et al. Transcriptome assemblies for studying sex-biased gene expression in the guppy, *Poecilia reticulata*. *BMC Genomics* 2014;15:400.
- [39] Sommer F, Bäckhed F. The gut microbiota—masters of host development and physiology. *Nat Rev Microbiol* 2013;11(4):227–38.
- [40] Tseng H-C, Fujimoto N, Ohnishi A. Characteristics of *Tepidimicrobium xylanilyticum* as a lactate-utilising bacterium in poly(lactic acid) decomposition during thermophilic anaerobic digestion. *Bioresour Technol Rep* 2020;12:100596.
- [41] Uren Webster TM, Rodriguez-Barreto D, Castaldo G, Gough P, Consuegra S, Garcia de Leaniz C. Environmental plasticity and colonisation history in the Atlantic salmon microbiome: a translocation experiment. *Mol Ecol* 2020;29(5):886–98.
- [42] Voigt A, Almaas E. Assessment of weighted topological overlap (wTO) to improve fidelity of gene co-expression networks. *BMC Bioinf* 2019;20(1):58.
- [43] Zilber-Rosenberg I, Rosenberg E. Role of microorganisms in the evolution of animals and plants: the hologenome theory of evolution. *FEMS Microbiol Rev* 2008;32(5):723–35.